provided by H. Bishop of the Department of Metallurgy, Cambridge).

The optical reflection transform method has a number of advantages over the normal metallographic examination of surfaces. Firstly, it provides a very rapid and easy detection of the presence of surface symmetries, especially for objects whose spacing is commensurate with the wavelength of light. Secondly, it enables a very rapid and quite accurate determination of the mean spacing of objects to be made. This is useful in analysing eutectic growth structures and measuring the inter-particle spacing. Thirdly, the technique is equally valid for small or large area (0.01 to 100 mm^2) examination.

Acknowledgements

The work described here was carried out at the Cavendish Laboratory, Cambridge and it is a pleasure to acknowledge the financial support provided by the National Physical Laboratory. It is also a pleasure to acknowledge the helpful discussions held with other members of the Metal Physics group of the Cavendish.

References

1. B. CHALMERS, *Proc. Phys. Soc.* **47** (1935) 733.
2. F. H. COCKS, B. N. DAS and G. A. WOLFF, *J. Mater. Sci.* **2** (1967) 470.
3. H. YAGI, K. SHIMAKAWA and N. TSUKADA, *Proc. IEEE* **57** (1969) 2156.

Received 5 September
and accepted 23 September 1974

DAVID R. CLARKE*
National Physical Laboratory
Teddington, Middlesex, UK

*Present address: Lawrence Berkeley Laboratory, University of California, Berkeley, California 94720, USA.

Density changes during creep of polycrystalline MgO

Cavities and cracks have been observed to form on grain boundaries during high temperature creep of ceramic materials [1-6]. However, this aspect of the creep behaviour of ceramics has received little attention compared with that devoted to the study of crack development during creep of metals and alloys [7, 8]. Furthermore, intercrystalline fracture of metallic materials has generally been studied using tensile creep conditions, whereas most of the work on creep of ceramics has been carried out using bend or compression testing procedures. In the present investigation, a technique which has frequently been employed to follow crack formation with metals, namely, the accurate measurement of density changes during creep [9-12], has been combined with microstructural studies in order to examine the development of grain-boundary cracks during compressive creep of polycrystalline MgO.

The present work was carried out using magnesia specimens (4.25 mm diameter and 6.4 mm long) having 94 to 96% theoretical density, 99.85% purity and 10 to 14 μm average grain diameter. Details of the material preparation [13], the constant stress creep equipment [14] and the differential weighing technique used to measure the specimen density [12] have been given elsewhere. With the small MgO specimens used, the fractional density change, $\Delta\rho/\rho$, could

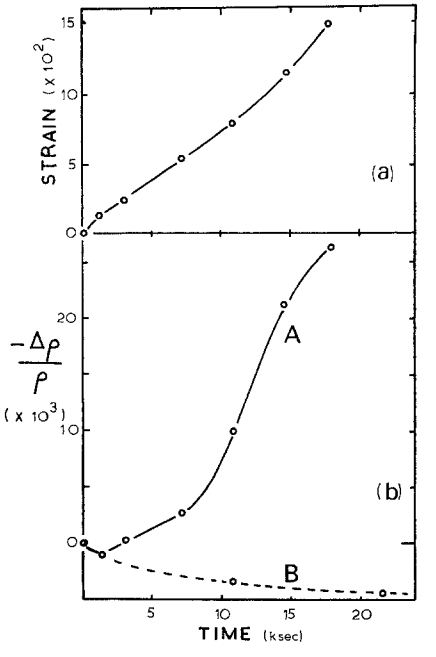

Figure 1 (a) Variation of creep strain with time for polycrystalline MgO at 96.2 MN m^{-2} and 1596 K. (O indicates points at which density determinations were carried out.) (b) Fractional change in specimen density with time at 1596 K during creep (curve A) and in the absence of an applied stress (curve B).

be determined only to 8×10^{-4} i.e. changes in porosity could be obtained reliably to about $\pm 0.1\%$.

In all cases, the creep tests were carried out in air at 1596 K under a stress of 96.2 MN m^{-2}. The variation of the true creep strain with time under these conditions is shown in Fig. 1a. The creep rate decreased continuously until a steady state was achieved, after which the creep rate accelerated at strains above $\sim 7\%$ when barrelling of the specimen just became detectable [14].

A microstructural examination was carried out on longitudinal sections prepared from a series of specimens which had been crept to various strains in the range 1 to 16%. At a strain of 2.3%, grain boundary cracking was just discernible. After $\sim 7\%$ strain, cracking was well developed, whereas after 16% strain, the cracks were large and beginning to join up (Fig. 2).

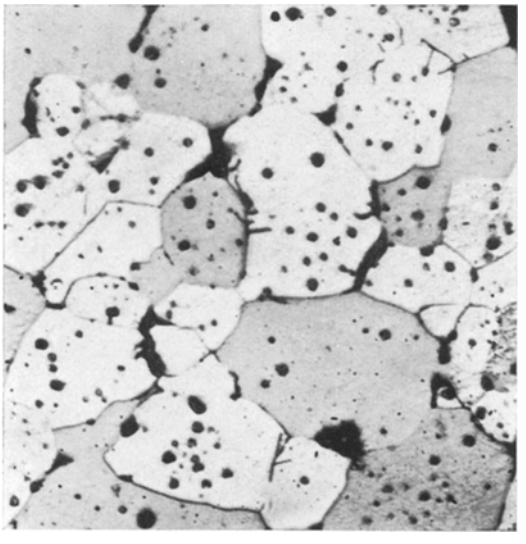

Figure 2 Grain-boundary crack development after $\sim 7\%$ creep strain in polycrystalline MgO at 96.2 MN m^{-2} and 1596 K (compression axis vertical). × 900

The majority of cracks occurred at triple points (where three grains meet), although cracks were also observed to form by the nucleation, growth and eventual coalescence of cavities on regions of the boundaries well away from triple points. Cracks were uniformly distributed throughout the specimens, except for a cone-shaped "dead-zone" extending from the specimen ends in

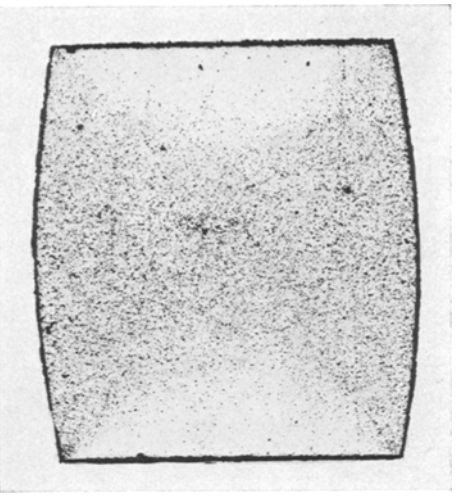

Figure 3 Longitudinal section of MgO specimen after 16% creep strain at 96.2 MN m^{-2} and 1596 K. × 10

which little or no cracking was evident (Fig. 3). This low incidence of cracking near the specimen ends is a consequence of frictional forces between the specimens and the platens affecting the deformation behaviour in this region. The overall incidence of cracking as a function of creep strain was assessed as the number of cracks per unit area (determined for regions of the specimens well away from the specimen ends). Isolated spherical voids, which may have been sinter pores present in the specimen initially, were not counted as cracks. It was estimated that, at strains of 2.3, 7 and 16%, the incidence of grain-boundary cracks was 100, 1800 and 2600 cracks per mm^2 respectively. Most of the cracks appeared to develop on boundaries approximately parallel to the stress axis. In order to quantify the crack distribution, the angle between each grain boundary and the compression axis was determined and the boundaries classified into groups at angle intervals of 10° from the direction of the applied stress on the polished longitudinal section of the specimen after $\sim 7\%$ creep strain. The proportion of boundaries on which cracks had developed was then established for each angle interval. The results (Fig. 4) show that the crack incidence was highest on boundaries parallel to the stress axis, indicating that cracks form preferentially on boundaries across which exists the maximum tensile stress.

The density of specimens prior to creep was found to vary from ~ 94 to $\sim 96\%$ of the

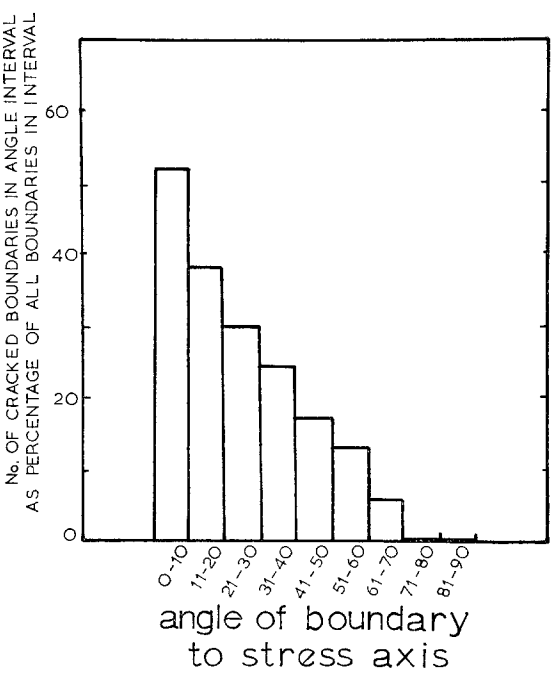

Figure 4 Percentage of grain boundaries on which cracks have developed as a function of the angle between the boundaries and the compression axis during creep of polycrystalline MgO at 96.2 MN m^{-2} and 1596 K.

theoretical value. To avoid the errors which would be introduced by using a number of specimens, the density variation during creep was measured on the same specimen throughout the entire creep curve. Then, to examine whether the specimen density was affected by sintering of cavities during the periods of heating to and cooling from the test temperature, the density of another specimen (of similar initial density) was measured as a function of time at 1596 K in the absence of an applied stress. During the creep test, after an initial increase in density early in the creep life, the specimen density decreased continuously, the rate of density decrease being greatest when barrelling of the specimen was detectable (Fig. 1b, curve A). In the absence of an applied stress, the density increased continuously with increasing sintering time, the rate of densification appearing to decrease with increasing time (Fig. 1b, curve B). The density changes occurring during sintering (Fig. 1b, curve B) were markedly lower than those observed under creep conditions (Fig. 1b, curve A), indicating that the heating and cooling periods involved with the interrupted creep test procedure used had little effect on the density as a function of creep strain.

Comparison of the densification which occurred early in the creep life (Fig. 1b, curve A) with that resulting from annealing in the absence of an applied stress (Fig. 1b, curve B) suggests that the initial increase in density under creep conditions was a result of sintering of pores initially present in the specimen prior to creep. However, the development of grain-boundary cracks rapidly offset the effects of sintering, leading to a decrease in density over most of the creep life.

The observed distribution of cracks with respect to the stress axis (Fig. 4) demonstrates the importance of the tensile stress across boundaries in the formation of cracks in MgO under creep conditions. The acceleration in the rate of density decrease at $\sim 7\%$ strain (Fig. 1b, curve A) then reflects the increase in tensile stress on boundaries parallel to the compression axis as barrelling becomes detectable. The observation that the incidence of cracking is highest on boundaries across which exists the greatest tensile stress has been established for metallic materials during high temperature creep tests carried out both in tension [15] and in compression [16]. Furthermore, the fracture appearance (Fig. 2), with cracks forming both at triple points and by the nucleation, growth and link-up of grain-boundary cavities, is typical of that observed for metals and alloys [6, 7]. These observations suggest that the mechanisms by which grain-boundary cavities and cracks develop in MgO are similar to those causing intercrystalline fracture with metallic materials.

References

1. L. E. POTEAT and C. S. YUST, *J. Amer. Ceram. Soc.* **49** (1966) 410.
2. P. E. EVANS, *ibid* **53** (1970) 365.
3. A. G. CROUCH, *ibid* **55** (1972) 558.
4. R. G. ST-JACQUES and R. ANGERS, *ibid* **55** (1972) 571.
5. C. K. L. DAVIES and S. K. SINHA-RAY, "Special Ceramics", Vol. 5 (British Ceram. Res. Ass., Stoke-on-Trent, 1972) p. 193.
6. A. CROSBY and P. E. EVANS, *J. Mater. Sci.* **8** (1973) 1573.
7. J. R. LOW, *Prog. Mat. Sci.* **12** (1963) 1.
8. A. J. PERRY, *J. Mater. Sci.* **9** (1974) 1016.
9. R. C. BOETTNER and W. D. ROBERTSON, *Trans. Met. Soc. AIME* **221** (1961) 613.
10. R. T. RATCLIFFE and G. W. GREENWOOD, *Phil. Mag.* **12** (1965) 59.

11. R. V. DAY, *J. Iron Steel Inst.* **203** (1965) 279.
12. P. BOWRING, P. W. DAVIES and B. WILSHIRE, *Metal Sci. J.* **2** (1968) 168.
13. D. R. F. SPENCER, *Trans. Brit. Ceram. Soc.* **11** (1973) 123.
14. J. M. BIRCH and B. WILSHIRE, *J. Mater. Sci.* **9** (1974) 794.
15. P. W. DAVIES, K. R. WILLIAMS and B. WILSHIRE, *Phil. Mag.* **18** (1968) 197.
16. P. W. DAVIES and R. DUTTON, *Acta Metallurgica* **15** (1967) 1365.

Received 30 September
and accepted 16 October 1974

J. M. BIRCH
P. J. KING
B. WILSHIRE
Department of Metallurgy and Materials Technology,
University College,
Singleton Park,
Swansea, UK

The rotation between selected area channelling patterns and micrographs in the SEM

Selected-area channelling patterns (SACPs) are now in wide use as a means of obtaining detailed crystallographic information from solid specimens in the scanning electron microscope (SEM) [1]. The best technique for generating these patterns is that described by van Essen *et al.* [2, 3]. In their method, the incident beam is made to rock about the selected area by deflecting the beam off-axis with a single set of scan coils, and then using the probe forming lens to bring the deflected rays back on to the axis. With this technique the minimum area from which a pattern can be obtained is set by the spherical aberration of the lens and the angle through which the beam is rocked. Areas as small as 1 μm diameter, for a total rock angle of 10° are attainable [4, 5].

When such patterns, generated by the deflection focusing technique, are used for crystallographic orientation determinations, it has been usually assumed that there is no relative rotation between the scan axes of the SACP and those of the normal micrograph. Such a rotation might be expected by analogy with that observed between diffraction patterns and micrographs in the transmission electron microscope. The rotation of the diffraction pattern is caused by the change in the intermediate lens excitation needed to go from diffraction to micrograph operation. In the SEM, however, the change from micrograph to SACP is made by simply switching off one set of scan coils. The lens excitation remains unchanged, and no apparent rotation would, therefore, be expected.

However, recent experimental work has established that, when this system is used on the Cambridge "Stereoscan", there is a rotation. This is made up of two components. The first is an inversion of 180°, and is a consequence of the change in scan direction (but not in scan angle) which occurs at the second scan pivot point. Both normal and selected-area channelling patterns are, therefore, inverted with respect to the micrograph. (The existence of this effect can readily be observed by noting that surface detail and channelling lines move in opposite senses during a rotation about the optic axis.) The second component is a variable rotation dependent on the working distance. Although this has been noted previously [6], no figures have been given for its magnitude. This can be measured in the following way. The SEM is set up in the electron-optical conditions used for SACPs. That is, a probe diameter of about 0.5 μm, a beam collimation of about 3×10^{-3} rad and an incident current of at least 10^{-9} A. A large single crystal (such as silicon) is then observed at $\times 20$ magnification. A conventional topographic image will be produced, together with an electron channelling pattern. With the specimen set normal to the optic axis of the microscope, the specimen is rotated so as to line up a band on the pattern with a line on the display screen (e.g. a "line-set" scan). The SEM is then switched to the SACP mode. The angle through which the specimen must now be rotated to bring the chosen band parallel once again to the line on the display screen is the required angle of rotation between the SCAP and the micrograph. Fig. 1 shows the result of this measurement as a function of the excitation of the final lens. The rotation is in a clockwise sense between the SACP and micrograph, and must be added to the 180° inversion.

This effect arises from the presence of stray fields in the back bore of the lens. The ray paths traversed by the beam through this region are different in the SACP and micrograph conditions.